Proxy reconstruction of ultraviolet-B irradiance at the Earth's surface, and its relationship with solar activity and ozone thickness

Journal Item

Proxy reconstruction of ultraviolet-B irradiance at the Earth's surface, and its relationship with solar activity and ozone thickness

P. E. Jardine[1,2], W. T. Fraser[3,2], W. D. Gosling[4,2], C. N. Roberts[5], W. J. Eastwood[6] and B. H. Lomax[7]

[1]Institute of Geology and Palaeontology, University of Münster, 48149 Münster, Germany.

[2]School of Environment, Earth and Ecosystem Sciences, The Open University, Walton Hall, Milton Keynes, MK7 6AA, UK.

[3]Geography, Department of Social Sciences, Oxford Brookes University, Oxford OX3 0BP, UK.

[4]Department of Ecosystem and Landscape Dynamics, Institute of Biodiversity & Ecosystem Dynamics (IBED), University of Amsterdam, 1090 GE Amsterdam, The Netherlands.

[5]School of Geography, Earth and Environmental Sciences, University of Plymouth, PL4 8AA, UK.

[6]School of Geography, Earth and Environmental Sciences, University of Birmingham, B15 2TT, UK.

[7]Agriculture and Environmental Science, University of Nottingham, Sutton Bonington Campus, Leicestershire, LE12 5RD, UK.

Corresponding author:

Phillip Jardine, Institute of Geology and Palaeontology, University of Münster, 48149 Münster, Germany.

Email: Phillip Jardine (jardine@uni-muenster.de).

Abstract

Solar ultraviolet-B (UV-B) irradiance that reaches the Earth's surface acts as a biotic stressor and has the potential to modify ecological and environmental functioning. The challenges of reconstructing UV irradiance prior to the satellite era mean that there is uncertainty over long-term surface UV-B patterns, especially in relation to variations in solar activity over centennial and millennial timescales. Here, we reconstruct surface UV-B irradiance over the last 650 years using a novel UV-B proxy based on the chemical signature of pollen grains. We demonstrate a statistically significant positive relationship between the abundance of UV-B absorbing compounds in *Pinus* pollen and modelled solar UV-B irradiance. These results show that trends in surface UV-B follow the overall solar activity pattern over centennial timescales, and that variations in solar output are the dominant control on surface level UV-B flux, rather than solar modulated changes in ozone thickness. The *Pinus* biochemical response demonstrated here confirms the potential for solar activity driven surface UV-B variations to impact upon terrestrial biotas and environments over long timescales.

Keywords: Ultraviolet-B irradiance; pollen; vegetation; palaeoclimate; solar activity; ozone

Introduction

The role of solar activity in influencing the Earth system has received an increase in attention over recent years (Ermolli et al., 2013; Gray et al., 2010; Solanki et al., 2013). Predominantly, the focus has been on total solar irradiance (TSI, defined as the amount of solar energy reaching the upper atmosphere) and its contributions to climatic changes versus anthropogenic inputs (Solanki et al., 2013). In addition to TSI, which affects temperature and atmospheric circulation patterns through 'bottom up' warming of the Earth's surface, there is a growing awareness of the importance of ultraviolet (UV) irradiance as a climate forcing mechanism (Gray et al., 2010; Ineson et al., 2015). UV irradiance stimulates production and

destruction of ozone via absorption driven processes (the Chapman cycle), resulting in a warming of the stratosphere and exerting a 'top down' influence on regional climatic and oceanic patterns through dynamical coupling with the underlying troposphere (Ermolli et al., 2013; Gray et al., 2010; Ineson et al., 2015; Solanki et al., 2013).

Solar UV-B (280-315 nm) radiation that reaches the Earth's surface (referred to hereafter as surface UV-B) is an important stressor on biotic systems, and has the potential to drive larger-scale ecosystem-level processes (Rozema et al., 1997). As well as directly damaging DNA, enhanced UV-B levels can lead to morphological and phenological changes in plants and possibly alter competitive relationships among species (Caldwell et al., 1998; Rozema et al., 1997). UV-B stimulates production of secondary metabolites that in part act as UV protective compounds, which are both a metabolic cost to the plant and can influence herbivory levels, plant decomposition and carbon cycling (Meijkamp et al., 1999; Rozema et al., 1997). Increased surface UV-B can also directly enhance leaf litter decomposition through photodegradation, and impact upon the activities of organisms such as animals, fungi and bacteria that play a role in decomposition and nutrient cycling (Gehrke et al., 1995; Rozema et al., 1997). While much attention has been focused on multidecadal increases in surface UV-B flux due to anthropogenic reductions in ozone thickness (Caldwell et al., 1998; Lomax et al., 2008), considerably less is known about the surface UV-B changes that result from long term (centuries to millennia) variations in solar activity, and what impact these have on ecological and environmental functioning.

Temporal changes in surface UV-B flux are a result of variations in solar UV irradiance, ozone thickness, and their interaction. Variations in solar activity have been characterized by satellite measurements since 1978 (all dates given in calendar years CE), and historical proxies such as sunspot counts from 1610 and cosmogenic radionuclides (primarily

^{10}Be and ^{14}C) through the Holocene (Solanki et al., 2013; Steinhilber et al., 2012; Svalgaard and Schatten, 2016). These indicators reveal solar cycles ranging in length from ~27 days to several millennia, as well as irregularly spaced, sustained 'Grand' minima and maxima of solar activity (e.g. the Maunder Minimum, ~1645 to 1710) (Solanki et al., 2013; Usoskin, 2017). Temporal variations in solar UV irradiance are still poorly understood, partly because of the discontinuous nature of spectral solar irradiance (SSI) satellite measurements (Haberreiter et al., 2017), but mostly because of the challenges of reconstructing UV irradiance beyond the satellite era. Nevertheless, SSI satellite measurements have revealed UV cycles (in particular the 11-year solar cycle) in phase with those of TSI (Usoskin, 2017), and the long term constancy of this relationship has been assumed in models of TSI and SSI such as the semi-empirical SATIRE-T model (Spectral And Total Irradiance REconstructions for the Telescope era), which has provided UV reconstructions back to the Maunder Minimum (Krivova et al., 2010), and the empirical NRLSSI2 model (Naval Research Laboratory Solar Spectral Irradiance), which has recently been extended back to 850 (Lean, 2018).

Increased UV-C (100-280 nm) flux during enhanced solar activity stimulates ozone production, limiting the flow of UV-B to the Earth surface. It follows that while incoming (top of atmosphere) UV-B and TSI may be correlated through time, surface level UV-B will be anticorrelated with both (Rampelotto et al., 2009; Rozema et al., 2002), and this is supported by ground based measurements of UV-B across the 11 year solar cycle (Rampelotto et al., 2009). Rozema et al. (2002) hypothesized that this relationship will be consistent across longer-term solar variations, with higher levels of surface UV-B flux during solar activity lows such as the Maunder Minimum, even though overall UV and TSI are reduced. Empirical evidence to test this hypothesis is currently lacking, however. Surface UV-B proxy reconstructions based on the abundance of photoprotective pigments in fossil

cladocera (water flea) carapaces in arctic and subarctic lakes (Nevalainen et al., 2015, 2016, 2018) demonstrated a positive correlation between surface UV-B and solar activity over the last millennium, which is the opposite pattern to that predicted by Rozema et al. (2002). However, UV-B proxies based on aquatic organisms such as cladocerans are influenced by water transparency as well as ambient UV-B, and so relate at least in part to local climatic and vegetation conditions and anthropogenic land use changes (Nevalainen et al., 2015, 2018). Although these impacts should have been limited in the arctic lake records used by Nevalainen et al. (2016), where water and UV transparency are high, it is still not clear what the long-term relationship between solar activity and surface UV-B is, and therefore what biotic and environmental impacts can be expected from solar variability in the future.

To address these uncertainties, we take advantage of a novel proxy for surface UV-B irradiance based on the chemistry of pollen grains (Fraser et al., 2014; Rozema et al., 2001; Seddon et al., 2019). Plants produce UV absorbing compounds (UACs) to protect their cells from the harmful effects of UV-B, and up-regulate production in response to increased UV-B doses (Fraser et al., 2014; Gao et al., 2004; Lomax et al., 2008; Rozema et al., 2001; Singh et al., 2014). Pollen grains and spores preserve well in the fossil record because their outer wall, or exine, is made of sporopollenin, a highly resistant biopolymer (Mackenzie et al., 2015). Critically, the UAC signal within the exine is also preserved (Jardine et al., 2016), and remains stable over geological time (Fraser et al., 2012). Therefore, by measuring the concentration of UACs in fossil and sub-fossil pollen grains, UV-B flux in the past can be reconstructed (Blokker et al., 2005, 2006; Fraser et al., 2014; Jardine et al., 2016; Lomax et al., 2008; Rozema et al. 2001; Seddon et al., 2019; Willis et al., 2011).

The UV-B response mechanism is thought to be an ancient evolutionary adaptation to terrestrial environments and occurs across the land plant phylogeny (Christie et al., 2012;

Jardine et al., 2016; Rizzini et al., 2011; Rozema et al., 1997), which means that a wide array of taxa are available for sampling from the pollen and spore record. To date, a positive correlation between UV-B and sporopollenin UAC levels has been demonstrated for *Lycopodium* (clubmoss) (Fraser et al., 2011; Jardine et al., 2016, 2017; Lomax et al., 2008, 2012; Watson et al., 2007), *Pinus* (pine) (Willis et al., 2011), *Cedrus atlantica* (Atlas cedar) (Bell et al., 2018), *Vicia faba* (broad or fava bean) (Rozema et al., 2001), and Poaceae (grasses) (Jardine et al., 2016), confirming the broad phylogenetic applicability of the UAC proxy. Furthermore, because this proxy is based on terrestrial plants, it is less biased by changes in the surrounding environment than those derived from aquatic organisms. UAC concentrations in pollen and spores are determined by the UV dose experienced by the parent plant, and are thought to represent the clear skies maximum UV level across the growing or pollen/spore production period (i.e. a timescale of several weeks prior to pollen/spore release) (Jardine et al., 2016; Lomax et al., 2012). The impact of short-term variations in cloudiness on UAC levels should therefore be limited, and inter-annual comparisons of UV-B flux can be achieved. Since the UAC proxy detects surface UV-B flux it is sensitive to changes in ozone column thickness (Lomax et al., 2008), which means that variations in surface-level UV-B caused by changes in ozone through time can be recovered.

Here, we use a maar lake sedimentary record from Nar Gölü in central Turkey, and analyse UAC concentrations in *Pinus* pollen to reconstruct surface UV-B flux over the last 650 years. This record is then used to test for the correlation between surface UV-B and modelled solar UV-B irradiance, following the assumption that TSI and solar UV-B irradiance will vary in phase though time. A negative correlation would support the hypothesis of Rozema et al. (2002), with solar activity highs leading to ozone production and decreased UV-B flux to the surface. A positive correlation would support the cladoceran UV-B reconstructions of Nevalainen et al., (2015, 2016, 2018), and would suggest that the

relationship between solar activity and ozone thickness observed on shorter timescales (e.g. Rampelotto et al., 2009) cannot simply be scaled up across centuries and millennia.

Materials and Methods

Nar Gölü (38°20'24"N, 34°27'23"E; 1363 m a.s.l.) is a maar lake in central Turkey, ~0.7 km^2 in area and ~26 m deep, with a sediment record extending through the Holocene and into the last glacial (Dean et al., 2015). The upper 2500 years of the sedimentary sequence is continuously annually laminated (varved), which has allowed for a precise chronology to be developed (Dean et al., 2015; Jones et al., 2005). The Nar Gölü sediment record has been the focus of previous sedimentological, mineralogical, palynological and geochemical research (Dean et al., 2013, 2015; England et al., 2008; Jones et al., 2005, 2006).

The sediment core used in this study was collected in 2001, and the pollen samples were initially documented in England et al. (2008). The age model for this core was based on varve counting, which was carried out independently by two workers, who recounted until agreement to within 3 laminae for each 6 cm section of core was reached (Jones et al., 2005). Replication of varve counts from additional cores has provided a maximum age uncertainty of 2.5% of the given age (Jones et al., 2006). The pollen samples were collected at ~20 year inter-sample resolution, with most samples representing 3 (sometimes 4 or 5) years of sediment accumulation. The whole sequence covers 640 years and ~160 cm of sediment core. The samples were processed according to standard palynological protocols, using 10% HCl, 10% NaOH, 60% HF, and acetolysis (England et al., 2008). We used the same pollen preparations in this study to maintain stratigraphic consistency with the pollen count data, and because standard processing protocols, including acetolysis (oxidation), do not impact upon the recoverability of variations in UAC concentrations across samples (Jardine et al., 2015,

181 2016, 2017). Furthermore, Bell (2018) showed that UAC levels were similar in acetolysed
182 and untreated *Pinus* pollen.
183
184 We selected *Pinus* as the target taxon because it is abundant through most of the upper
185 part of the Nar Gölü record, with relative abundances of 13% to 45% of the pollen sum and
186 influx rates of 300 to 4400 cm^2/year (England et al., 2008). Furthermore, compared to lower
187 stature vegetation the impact of localized shading on UV reconstructions (Fraser et al., 2011;
188 Jardine et al., 2016) should be minimal. A positive association between UAC levels and UV-
189 B has also previously been demonstrated for *Pinus* pollen, across both a modern latitudinal
190 gradient and over the last 9.5 kyr (Willis et al., 2011), suggesting that a measurable signal is
191 recoverable from the Nar Gölü *Pinus* pollen record. *Pinus* pollen within the Nar Gölü
192 sediments represents mostly regional rather than local vegetation, and is mostly derived from
193 the Taurus Mountains >70 km south and southeast of Nar Gölü, although *Pinus* was also
194 planted near the lake in the 1980s (England et al., 2008). In the modern day, the three main
195 *Pinus* species in this region are *Pinus brutia*, *Pinus nigra* and *Pinus sylvestris* (Woldring and
196 Bottema, 2003), and these are anticipated to have been the major contributors to the Nar Gölü
197 *Pinus* pollen record during the study interval.
198
199 We used Fourier Transform Infrared (FTIR) microspectroscopy to generate the
200 chemical data, because previous analyses (Bell et al., 2018; Fraser et al., 2011; Jardine et al.,
201 2016, 2017; Lomax et al., 2008, 2012; Watson et al., 2007) have shown that this can
202 successfully capture variations in UAC abundances at small sample sizes. To prepare the
203 samples for FTIR analysis, individual *Pinus* pollen grains were picked out from the processed
204 sediment samples and mounted on ZnSe windows. To pick the pollen grains we used an
205 inverted microscope with a micromanipulator attachment, the full set-up comprising
206 Narishige MMN-1 and MMO-202ND course and fine control micromanipulators, an IM-11-2

pneumatic microinjector, with a Microtec IM-2 inverted microscope. The picked pollen grains were arranged in groups of 4 to 5 grains on the ZnSe windows, with 5 replicate groups per sample. This means that each FTIR spectrum represents 4 or 5 pollen grains, and each pollen sample is represented by 5 replicate FTIR spectra. We generated the data using a Thermo Scientific (Waltham, MA, USA) Nicolet Nexus FTIR bench unit connected to a Continuum IR microscope fitted with an MCT-A liquid nitrogen-cooled detector and a Reflachromat 15x objective lens. FTIR spectra were generated in transmission mode using a microscope aperture of 100 x 100 μm recording the mean of 256 scans with a resolution of 1.928 cm^{-1} wavenumbers. Five of the 33 samples in the study interval had insufficient *Pinus* pollen for FTIR analysis, resulting in a dataset of 28 samples.

Peak height measurement and data analysis were carried out in R v3.4.0 (R Core Team, 2017). The package 'baseline' v1.2-1 (Liland and Mevik, 2015) was used to baseline correct the IR spectra, by subtracting a 2nd order polynomial baseline from each spectrum (Figure 1). We quantified UAC concentrations by measuring the height of the 1510 cm^{-1} aromatic (C=C) peak (Fig. 1), because this peak records changes in the abundance of the phenolic compounds *para*-coumaric acid and ferulic acid that act as UACs in sporopollenin (Fraser et al., 2014; Watson et al., 2007). Absorbance values in IR spectra relate to the thickness of material being analysed, so following previous research (Fraser et al., 2011; Jardine et al., 2015, 2016, 2017; Lomax et al., 2008, 2012) the 1510 cm^{-1} aromatic peak height was normalized against the hydroxyl (OH) band centred on 3300 cm^{-1} (Figure 1). Although the aromatic/OH ratio has not yet been calibrated to UAC concentrations or UV levels, it does provide a successful proxy whereby higher aromatic/OH ratio values equate to higher UV-B flux (Fraser et al., 2011; Jardine et al., 2016, 2017; Lomax et al., 2008, 2012). Short-term variations in ambient UV-B flux experienced by the pollen-producing plants will add noise to the UAC reconstruction; possible sources of additional variability are considered

in the Discussion. The raw data (sample ages and peak height measurements) are available for download from figshare (Jardine et al., 2019). **[NB For review please used this private link to access the data: https://figshare.com/s/45c1f29f1d76c1cbc01d].**

[Insert Figure 1]

We used the historical SSI reconstruction of Lean (2018) to obtain solar UV-B irradiance estimates for the last 650 years. This SSI reconstruction covers the period 850 to 2016, and provides an annually resolved time series that incorporates information from space-based irradiance observations, sunspots and cosmogenic radionuclides (full details in Lean 2018). Within the ultraviolet the SSI estimates are resolved to 1 nm wavebands. We therefore integrated the irradiance values within the range 280 to 315 nm, to obtain an irradiance reconstruction integrated across the UV-B part of the solar spectrum (shown in Figure 2b).

We used Spearman's rank order correlation to test the association between UACs and solar UV-B. For the UACs we used the mean of the five replicates within each pollen sample, and for solar UV-B we used the mean UV-B irradiance values within the calendar years represented by each pollen sample. Spearman's rank order correlation is appropriate because it is a non-parametric test that does not assume normality of distributions or a linear relationship among variables. To examine the influence of shared long-term temporal trends among the variables, we detrended the data by taking the residuals from linear regressions of each variable against time. The residuals were then used as variables in the correlation test.

Results

The Nar Gölü *Pinus* UAC record (Figure 2a) shows that surface level UV-B irradiance has varied over the last 650 years. Visual comparison with the solar UV-B reconstruction of

Lean (2018) (Figure 2b) reveals many of the same features, including an initial high value at ~ 1350, minima at ~1460 to 1550 (the Spörer Minimum), 1645 to 1710 (the Maunder Minimum), ~1790 to 1820 (the Dalton Minimum), and 1880 to 1920, and the rise from the Maunder Minimum to the late 20th Century. The Spearman's rank order correlation between the UAC data and solar UV-B reconstruction demonstrates statistically significant positive relationships for both raw (n = 28, r_s = 0.52, p = 0.005) and detrended datasets (n = 28, r_s = 0.55, p = 0.004) (Figure 3). These correlations show that the visual similarities between the surface and solar UV-B data are robust.

[Insert Figure 2]

[Insert Figure 3]

Discussion

Our results show a positive correlation between the *Pinus* UAC data and the solar UV-B reconstruction of Lean (2018), demonstrating that solar activity and surface UV-B trends have been concordant over the last 650 years. These results are in agreement with the cladoceran-based surface UV-B reconstructions of Nevalainen et al. (2015, 2016, 2018), but are not consistent with the hypothesis of Rozema et al. (2002) that surface level UV-B should be anti-correlated with solar activity across grand solar minima and maxima. Our results therefore suggest that any variations in the thickness of the ozone layer were not sufficient to alter the incoming UV-B flux.

These results also demonstrate that the anti-correlation between solar activity and ground-based measurements of UV across the 11 year solar cycle (Rampelotto et al., 2009) cannot simply be scaled up to longer timescales (Rozema et al., 2002). Whether this implies a

different relationship between solar activity, UV and ozone thickness across the 11 year solar cycle and longer-term cycles and trends is currently unclear. While solar UV irradiance at wavelengths under 242 nm leads to ozone production, longer wavelength UV destroys it (Ball et al., 2016), therefore given the right balance of change across the UV spectrum decreases in ozone creation across solar minima could be cancelled out by decreases in ozone destruction (and vice versa during solar maxima). Ozone concentrations are also modulated by hydrogen, nitrogen, and chlorine catalytic cycles (Lary, 1997), and long-term variations in the atmospheric concentrations of HOx, NOx and ClOx radicals may influence how ozone thickness changes in response to solar UV. This question deserves further research, both with more instrumental measurements of spectral UV irradiance and surface level UV-B, and additional high-resolution UAC-based records over longer timescales.

While the relationships between our UAC data and solar UV-B are statistically significant (Figure 3), the strength of the correlations are moderate (r_s = 0.52 for the raw data, and r_s = 0.55 for the detrended data). In the Nar Gölü record we have identified three main factors that, in addition to solar UV-B, may have been responsible for variation in the UAC signal. First, the *Pinus* pollen does not represent local vegetation, but is thought to be largely sourced from the Taurus Mountains (England et al., 2008). The pollen signal therefore likely represents a mix of altitudes and incoming UV-B levels (Lomax et al., 2012), which will contribute to within-sample variance (Seddon et al., 2019). To the extent that the UV-B response differs among the *Pinus* species contributing pollen to the Nar Gölü record, any variations in their relative abundances over time may have added further noise to the UAC signal. The recently planted *Pinus* trees near Nar Gölü (England et al., 2008) may also have impacted upon the UAC measurement from the most recent sample in the record, which covers the years 1998 to 2001.

Second, variations in cloud cover modify surface UV irradiance levels (Calbó et al., 2005; Fraser et al., 2011). Although the UAC proxy is unlikely to be affected by short-term variations in cloudiness (Lomax et al., 2012), interannual variability in cloud cover may add additional noise to UAC time series where each sample represents several years of pollen release.

Third, any errors in the sediment core chronology will add noise to the correlations. Although dating precision in the Nar Gölü record is thought to be better than the maximum age uncertainty of 2.5% would suggest (Dean et al., 2013), small errors are likely to be inevitable even in continuously varved sediments, and the magnitude of change in solar UV-B irradiance across the 11 year solar cycle (Figure 2b; Lean, 2018) suggests that age model deviations could add substantial noise to the UAC-UV relationship. While dating errors of a few years could artificially impose a positive correlation between the solar UV-B reconstruction and UAC data, the sustained, multi-decadal solar UV-B lows during both the Spörer Minimum and Maunder Minimum (Figure 2b) coincide with intervals of low UAC concentrations (Figure 2a). This suggests that the positive correlation demonstrated here is not an artefact of minor errors in the varve chronology, but rather represents a genuine signal.

Despite these sources of variability, the UAC proxy has successfully recovered the major solar UV-B signal, demonstrating that it has much to offer as a means of examining solar inputs to the Earth system and their contributions to biotic and climatic change. As a surface UV-B proxy UAC measurements allow us to test hypotheses relating to changes in ozone thickness through time (Lomax et al., 2008), and can aid in deconvoluting the effects of solar activity and ozone-related variations on UV-B at the Earth's surface. The pollen UAC proxy could also be used in conjunction with UV proxies based on aquatic organisms (Nevalainen et al., 2016) to separate out solar UV from water transparency effects

(Nevalainen et al., 2015, 2018), and therefore constrain key factors impacting on aquatic ecosystems. More generally, the UAC proxy can be used to test for the impacts of surface UV-B changes on biotic systems, in relation to solar UV irradiance variations, longer term cycles in the Earth's orbit around the Sun (Jardine et al., 2016), and periods of ozone layer disruption (Lomax et al., 2008; Visscher et al., 2004).

Our *Pinus* UAC data, taken together with the cladocera data of Nevalainen et al. (2015, 2016, 2018), demonstrate that variations in solar UV irradiance are sufficient to drive biochemical responses in disparate environments and groups of organisms. Future changes in surface UV-B flux, whether driven by variations in solar activity or atmospheric composition, will alter not just organismal stress but also the metabolic costs of producing UV protective compounds, and may influence interspecific competitive relationships and ecosystem-level processes such as decomposition and carbon cycling (Rozema et al., 1997). The relative importance of these responses therefore needs to be assessed in future studies of ecological change.

Conclusions

We have provided the first detailed proxy reconstruction of surface level UV-B flux on centennial timescales. By linking this with a published solar UV-B reconstruction, we have shown that solar UV-B flux at the surface follows a similar long-term trend to top of atmosphere UV-B. On the timescales considered here, incoming solar UV flux will therefore be the dominant control on surface-level UV, rather than UV modulated ozone thickness. In addition to better understanding and modelling sources of variance in UAC reconstructions, future research in this area needs to focus on calibrating the UAC UV-B proxy to a specific dose-response relationship, to quantify the magnitude of change across different timescales (Rozema et al., 2001, 2002, 2009; Seddon et al., 2019). Developing an action spectrum

(Herman, 2010; Rozema et al., 2001; Seddon et al., 2019) for UAC production will also be important for quantifying how UAC concentrations vary with changes in ozone levels. Together, these measures will help towards understanding how variations in solar UV irradiance impact on Earth's climate and biota through time, both in the past and in the future.

Acknowledgements

The raw data for this study are available on figshare: https://dx.doi.org/10.6084/m9.figshare.8075519 **[NB For review please used this private link to access the data: https://figshare.com/s/45c1f29f1d76c1cbc01d].** We thank NERC (grant NE/K005294/1) for funding this research, and a previous NERC award (NER/S/A/2002/10316) to University of Birmingham-based PhD student, Ann England. Andy Moss is thanked for lab support. We also thank Benjamin Bell and Liisa Nevalainen for insightful reviews, and the anonymous reviewers whose comments improved earlier versions of this paper.

References

Ball WT, Haigh JD, Rozanov EV, et al. (2016) High solar cycle spectral variations inconsistent with stratospheric ozone observations. *Nature Geoscience* 9: 206-209.

Bell, BA. (2018) *Advancing the Application of Analytical Techniques in the Biological Chemistry of Sporopollenin: Towards Novel Plant Physiological Tracers in Quaternary Palynology*. PhD Thesis, University of Manchester, UK.

Bell BA, Fletcher WJ, Ryan P, et al. (2018) UV-B-absorbing compounds in modern *Cedrus atlantica* pollen: The potential for a summer UV-B proxy for Northwest Africa. *The Holocene* 28: 1382-1394.

Blokker, P, Boelen, P, Broekman, R and Rozema, J. (2006) The occurrence of *p*-coumaric acid and ferulic acid in fossil plant materials and their use as UV-proxy. *Plant Ecology* 182: 197-207.

Blokker, P, Yeloff, D, Boelen, P, Broekman, R and Rozema, J. (2005). Development of a proxy for past surface UV-B irradiation: A thermally assisted hydrolysis and methylation py-GC/MS method for the analysis of pollen and spores. *Analytical Chemistry* 77: 6026-6031.

Calbó J, Pagès D and González J-A. (2005) Empirical studies of cloud effects on UV radiation: A review. *Reviews of Geophysics* 43.

Caldwell MM, Björn LO, Bornman JF, et al. (1998) Effects of increased solar ultraviolet radiation on terrestrial ecosystems. *Journal of Photochemistry and Photobiology B: Biology* 46: 40-52.

Christie JM, Arvai AS, Baxter KJ, et al. (2012) Plant UVR8 photoreceptor senses UV-B by tryptophan-mediated disruption of cross-dimer salt bridges. *Science* 335: 1492-1496.

Dean JR, Jones MD, Leng MJ, et al. (2015) Eastern Mediterranean hydroclimate over the late glacial and Holocene, reconstructed from the sediments of Nar lake, central Turkey, using stable isotopes and carbonate mineralogy. *Quaternary Science Reviews* 124: 162-174.

Dean JR, Jones MD, Leng MJ, et al. (2013) Palaeo-seasonality of the last two millennia reconstructed from the oxygen isotope composition of carbonates and diatom silica from Nar Gölü, central Turkey. *Quaternary Science Reviews* 66: 35-44.

England A, Eastwood WJ, Roberts CN, et al. (2008) Historical landscape change in Cappadocia (central Turkey): a palaeoecological investigation of annually laminated sediments from Nar lake. *The Holocene* 18: 1229-1245.

411 Ermolli I, Matthes K, Dudok de Wit T, et al. (2013) Recent variability of the solar spectral
412 irradiance and its impact on climate modelling. *Atmospheric Chemistry and Physics*
413 13: 3945-3977.
414 Fraser WT, Lomax BH, Jardine PE, et al. (2014) Pollen and spores as a passive monitor of
415 ultraviolet radiation. *Frontiers in Ecology and Evolution* 2.
416 Fraser WT, Scott AC, Forbes AES, et al. (2012) Evolutionary stasis of sporopollenin
417 biochemistry revealed by unaltered Pennsylvanian spores. *New Phytologist* 196: 397-
418 401.
419 Fraser WT, Sephton MA, Watson JS, et al. (2011) UV-B absorbing pigments in spores:
420 biochemical responses to shade in a high-latitude birch forest and implications for
421 sporopollenin-based proxies of past environmental change. *Polar Research* 30: 8312.
422 Gao W, Zheng Y, Slusser JR, et al. (2004) Effects of Supplementary Ultraviolet-B lrradiance
423 on Maize Yield and Qualities: A Field Experiment. *Photochemistry and Photobiology*
424 80: 127-131.
425 Gehrke C, Johanson U, Callaghan TV, et al. (1995) The impact of enhanced ultraviolet-B
426 radiation on litter quality and decomposition processes in *Vaccinium* leaves from the
427 Subarctic. *Oikos* 72: 213-222.
428 Gray LJ, Beer J, Geller M, et al. (2010) Solar Influences on Climate. *Reviews of Geophysics*
429 48.
430 Haberreiter M, Schöll M, Dudok de Wit T, et al. (2017) A new observational solar irradiance
431 composite. *Journal of Geophysical Research: Space Physics* 122: 5910-5930.
432 Herman JR. (2010) Use of an improved radiation amplification factor to estimate the effect of
433 total ozone changes on action spectrum weighted irradiances and an instrument
434 response function. *Journal of Geophysical Research* 115.
435 Ineson S, Maycock AC, Gray LJ, et al. (2015) Regional climate impacts of a possible future
436 grand solar minimum. *Nature Communications* 6: 7535.

437 Jardine PE, Abernethy FAJ, Lomax BH, et al. (2017) Shedding light on sporopollenin
438 chemistry, with reference to UV reconstructions. *Review of Palaeobotany and*
439 *Palynology* 238: 1-6.
440 Jardine PE, Fraser, WT, Gosling, WD, et al. (2019) Data from "Reconstruction of ultraviolet-
441 B irradiance at the Earth's surface, and its relationship with solar activity and ozone
442 thickness". figshare, https://dx.doi.org/10.6084/m9.figshare.8075519.
443 Jardine PE, Fraser WT, Lomax BH, et al. (2015) The impact of oxidation on spore and pollen
444 chemistry. *Journal of Micropalaeontology* 34: 139-149.
445 Jardine PE, Fraser WT, Lomax BH, et al. (2016) Pollen and spores as biological recorders of
446 past ultraviolet irradiance. *Scientific Reports* 6: 1-8.
447 Jones MD, Leng MJ, Roberts CN, et al. (2005) A Coupled Calibration and Modelling
448 Approach to the Understanding of Dry-Land Lake Oxygen Isotope Records. *Journal*
449 *of Paleolimnology* 34: 391-411.
450 Jones MD, Roberts CN, Leng MJ, et al. (2006) A high-resolution late Holocene lake isotope
451 record from Turkey and links to North Atlantic and monsoon climate. *Geology* 34:
452 361.
453 Krivova NA, Vieira LEA and Solanki SK. (2010) Reconstruction of solar spectral irradiance
454 since the Maunder minimum. *Journal of Geophysical Research* 115.
455 Lary DJ. (1997) Catalytic destruction of stratospheric ozone. *Journal of Geophysical*
456 *Research: Atmospheres* 102: 21515-21526.
457 Lean JL. (2018) Estimating Solar Irradiance Since 850 CE. *Earth and Space Science* 5: 133-
458 149.
459 Liland KH and Mevik B-H. (2015) baseline: Baseline Correction of Spectra. 1.2-1 ed.
460 Lomax BH, Fraser WT, Harrington G, et al. (2012) A novel palaeoaltimetry proxy based on
461 spore and pollen wall chemistry. *Earth and Planetary Science Letters* 353-354: 22-28.

462 Lomax BH, Fraser WT, Sephton MA, et al. (2008) Plant spore walls as a record of long-term
463 changes in ultraviolet-B radiation. *Nature Geoscience* 1: 592-596.
464 Mackenzie G, Boa AN, Diego-Taboada A, et al. (2015) Sporopollenin, The Least Known Yet
465 Toughest Natural Biopolymer. *Frontiers in Materials* 2: 1-5.
466 Meijkamp B, Aerts R, van de Staaij J, et al. (1999) Effects of UV-B on secondary metabolites
467 in plants. In: Rozema J (ed) *Stratospheric ozone depletion: The effects of enhanced*
468 *UV-B on terrestrial ecosystems.* Leiden: Backhuys, 71-99.
469 Nevalainen L, Luoto TP, Rantala MV, et al. (2015) Role of terrestrial carbon in aquatic UV
470 exposure and photoprotective pigmentation of meiofauna in subarctic lakes.
471 *Freshwater Biology* 60: 2435-2444.
472 Nevalainen L, Rantala MV, Luoto TP, et al. (2016) Long-term changes in pigmentation of
473 arctic Daphnia provide potential for reconstructing aquatic UV exposure. *Quaternary*
474 *Science Reviews* 144: 44-50.
475 Nevalainen L, Rantala MV, Rautio M, et al. (2018) Spatio-temporal cladoceran
476 (Branchiopoda) responses to climate change and solar radiation in subarctic ecotonal
477 lakes. *Journal of Biogeography* 45: 1954-1965.
478 Rampelotto PH, da Rosa MB and Schuch NJ. (2009) Solar cycle and UV‐B comparison for
479 South America−South of Brazil (29° S, 53° W). In: Nakajima T and Yamasoe MA
480 (eds) *AIP Conference Proceedings.* AIP, 490-493.
481 R Core Team (2017) R: A language and environment for statistical computing. 3.4.2 ed.
482 Vienna, Austria: R Foundation for Statistical Computing.
483 Rizzini L, Favory JJ, Cloix C, et al. (2011) Perception of UV-B by the *Arabidopsis* UVR8
484 Protein. *Science* 332: 103-106.
485 Rozema J, Blokker P, Mayoral Fuertes MA, et al. (2009) UV-B absorbing compounds in
486 present-day and fossil pollen, spores, cuticles, seed coats and wood: evaluation of a

487 proxy for solar UV radiation. *Photochemical and Photobiological Sciences* 8: 1233-
488 1243.
489 Rozema J, Broekman RA, Blokker P, et al. (2001) UV-B absorbance and UV-B absorbing
490 compounds (*para*-coumaric acid) in pollen and sporopollenin: the perspective to track
491 historic UV-B levels. *Journal of Photochemistry and Photobiology B: Biology* 62:
492 108-117.
493 Rozema J, van de Staij J, Björn L-O, et al. (1997) UV-B as an environmental factor in plant
494 life: stress and regulation. *Trends in Ecology and Evolution* 12: 22-28.
495 Rozema J, van Geel B, Björn L-O, et al. (2002) Toward Solving the UV Puzzle. *Science* 296:
496 1621-1622.
497 Seddon AWR, Festi D, Robson TM, et al. (2019) Fossil pollen and spores as a tool for
498 reconstructing ancient solar-ultraviolet irradiance received by plants: an assessment of
499 prospects and challenges using proxy-system modelling. *Photochemical and*
500 *Photobiological Sciences* 18: 275-294.
501 Singh SK, Reddy KR, Reddy VR, et al. (2014) Maize growth and developmental responses to
502 temperature and ultraviolet-B radiation interaction. *Photosynthetica* 52: 262-271.
503 Solanki SK, Krivova NA and Haigh JD. (2013) Solar Irradiance Variability and Climate.
504 *Annual Review of Astronomy and Astrophysics* 51: 311-351.
505 Steinhilber F, Abreu JA, Beer J, et al. (2012) 9,400 years of cosmic radiation and solar
506 activity from ice cores and tree rings. *Proceedings of the National Academy of*
507 *Sciences* 109: 5967-5971.
508 Svalgaard L and Schatten KH. (2016) Reconstruction of the Sunspot Group Number: The
509 Backbone Method. *Solar Physics* 291: 2653-2684.
510 Usoskin IG. (2017) A history of solar activity over millennia. *Living Reviews in Solar Physics*
511 14.

512 Visscher H, Looy CV, Collinson ME, et al. (2004) Environmental mutagenesis during the
513 end-Permian ecological crisis. *Proceedings of the National Academy of Sciences of the*
514 *United States of America* 101: 12952-12956.
515 Watson JS, Septhon MA, Sephton SV, et al. (2007) Rapid determination of spore chemistry
516 using thermochemolysis gas chromatography-mass spectrometry and micro-Fourier
517 transform infrared spectroscopy. *Photochemical and Photobiological Sciences* 6: 689-
518 694.
519 Willis KJ, Feurdean A, Birks HJB, et al. (2011) Quantification of UV-B flux through time
520 using UV-B-absorbing compounds contained in fossil Pinus sporopollenin. *New*
521 *Phytologist* 192: 553-560.
522 Woldring, H and Bottema, S. (2003) The vegetation history of east-central Anatolia in
523 relation to Archaeology: the Eski Acégöl pollen evidence compared with the Near
524 Eastern environment. *Palaeohistoria* 43/44: 1-31.
525

Figures

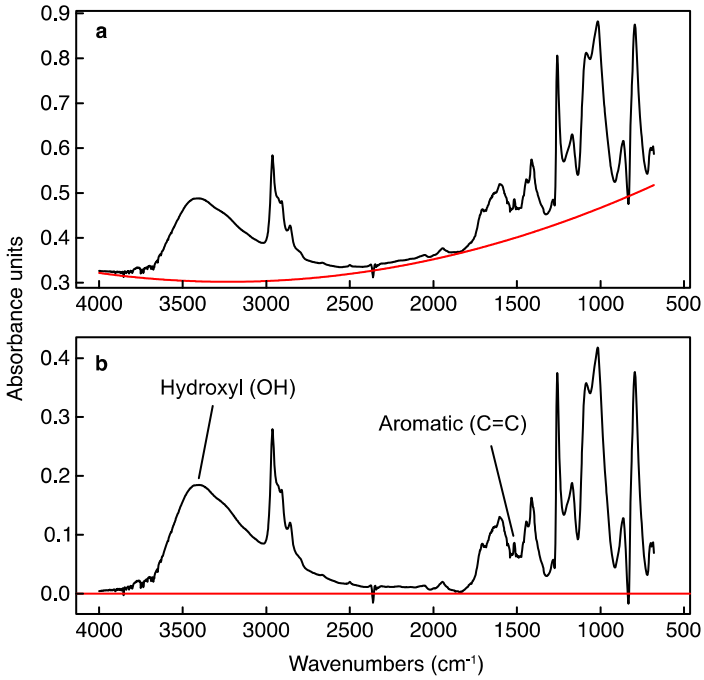

Figure 1. Representative chemical spectra of Nar Gölü *Pinus* pollen, from a sample dating from 1741 CE. (a) uncorrected spectrum showing fitted 2nd order polynomial baseline. (b) baseline corrected spectrum. The 1510 cm^{-1} aromatic peak represents UV-B absorbing compounds (UACs) within pollen grains, and the 3300 cm^{-1} hydroxyl band is used to normalize the peak height measurement.

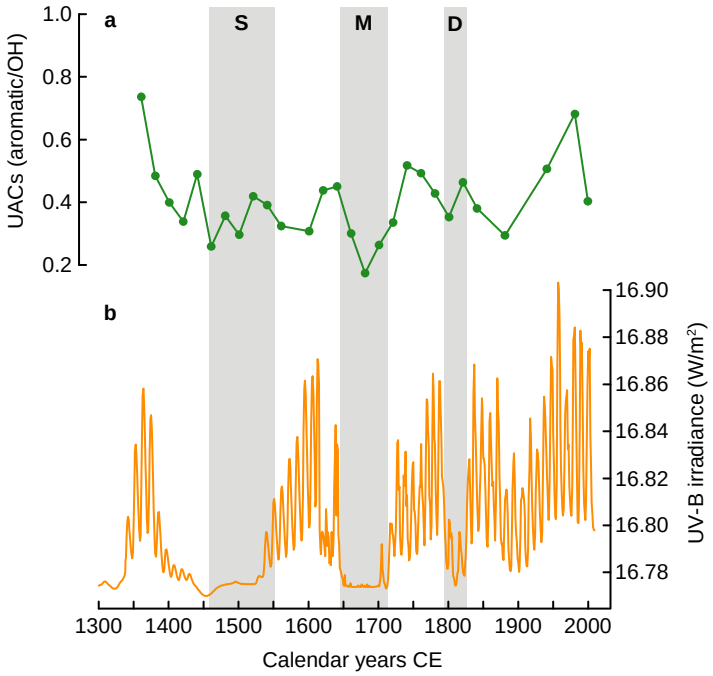

534

535 **Figure 2.** Surface and solar UV-B records. (a) Pinus UAC data from Nar Gölü, shown as the
536 mean of five replicates (solid green line with points showing samples) ±1 standard deviation
537 (shaded area). (b) Modeled solar UV-B irradiance, from Lean (2018). Grey shaded regions
538 show solar minima, D = Dalton Minimum, M = Maunder Minimum, S = Spörer Minimum.

539

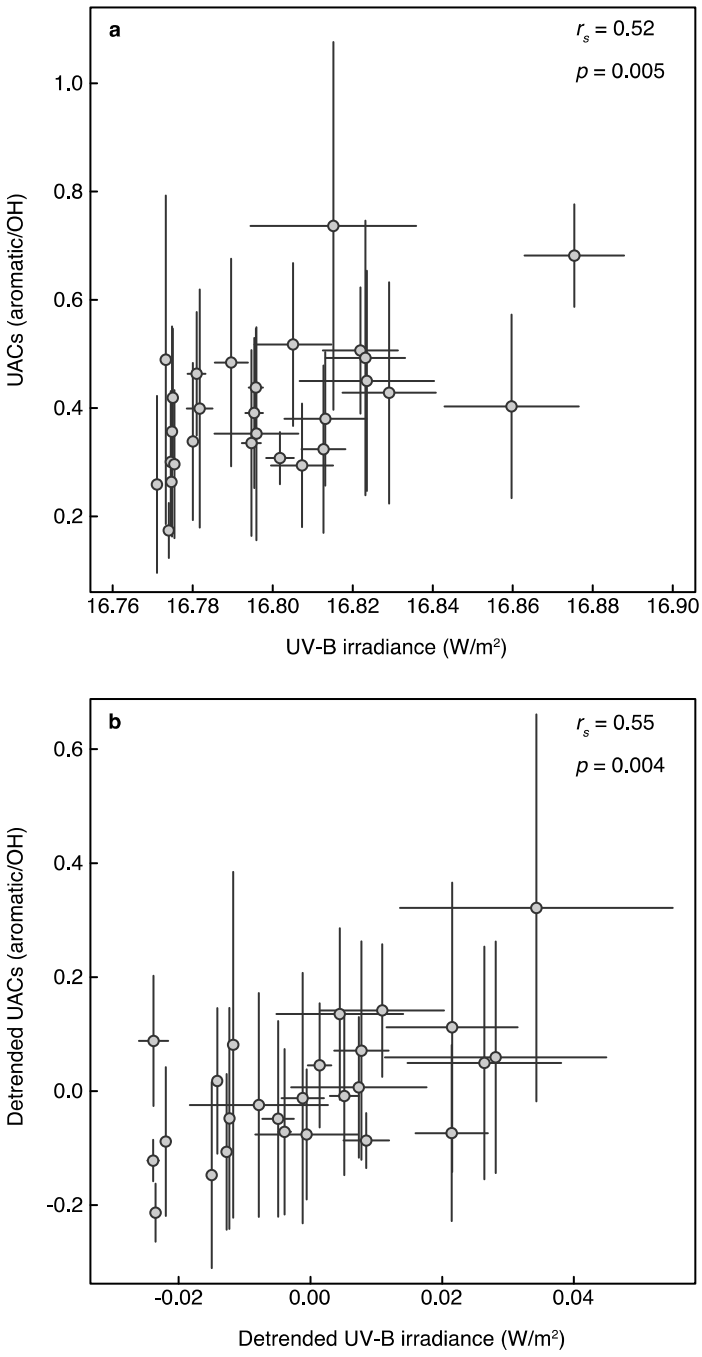

Figure 3. *Pinus* UAC data plotted against modeled solar UV-B irradiance (Lean 2018), for both raw (a) and detrended (b) data. For the UAC data, the points show the mean of five replicates, and the error bars are 1 standard deviation. For the UV-B irradiance reconstruction, the points are the mean values within the calendar years represented by each pollen sample, and the error bars are 1 standard deviation. r_s = Spearman's rank order correlation coefficient, p = p value of correlation.